Polymer Bulletin (2024) 81:4407–4426
https://doi.org/10.1007/s00289-023-04920-4

ORIGINAL PAPER

Graphene oxide enhanced hydrogel as an adsorbent for effective removal of methylene blue

Yunxiang Zheng[1] · **Lina Zong**[1] · **Xiangpeng Wang**[1]

Received: 26 February 2023 / Revised: 1 July 2023 / Accepted: 17 July 2023 /
Published online: 26 July 2023

Abstract

When used to treat printing and dyeing effluents, the existing hydrogels have the following problems: limited mechanical strength, slow adsorption rate, and poor reusability. Therefore, a simple one-pot method was used to prepare poly (acrylic acid-2-acrylamide-2-methyl-1-propanesulfonic acid)-g-sodium alginate/graphene oxide (P(AA-AMPS)/SA-GO) composite hydrogel, which was analyzed by Fourier transform infrared, scanning electron microscope, confocal laser scanning microscope and Brunauer–Emmet–Teller method. The mechanical properties, swelling ratios and adsorption performance of the composite hydrogel were determined in detail. The results show that the composite hydrogel has a porous structure and excellent mechanical properties. The maximum elongation at break and tensile strength can reach 803% and 104.8 kPa, respectively. When the GO content is 1.2%, the swelling ratio and methylene blue (MB) adsorption capacity are the highest, 54.9 g/g and 486.5 mg/g, respectively. The external conditions have a significant effect on the adsorption performance of the hydrogel. When the adsorption conditions are as follows: the adsorption temperature is 25 ℃, the amount of hydrogel is 0.1 g, the pH is 8, and the initial concentration of MB is 500 mg/L, the highest removal efficiency of MB is 98.1% in 90 min. Coexisting ions can inhibit the removal of MB. The adsorption model fitting and kinetic analyses show that P(AA-AMPS)/SA-GO follows the Langmuir adsorption model and belongs to single-layer adsorption. The adsorption kinetic model study shows that the gel fits the quasi-second-order kinetic model, with chemical adsorption as the primary and physical adsorption as the auxiliary. The P(AA-AMPS)/SA-GO hydrogel has a remarkable adsorption effect on methylene blue wastewater and can be used as an efficient adsorbent for wastewater treatment.

Keywords Graphene oxide · Enhanced hydrogel · Methylene blue · Adsorption · Porous · Mechanical strength

Extended author information available on the last page of the article

Introduction

With the rapid development of the modern printing and dyeing industry, the water pollution caused by the discharge of dye wastewater is becoming increasingly severe [1]. Dye wastewater has the characteristics of complex composition, high organic concentration and chroma, and difficult biodegradation [2, 3]. How to treat printing and dyeing wastewater has become a focus of attention. Many methods exist to solve this problem, such as adsorption, biodegradation, photocatalysis, ion exchange, and membrane filtration [4]. Among them, the adsorption method has the characteristics of low cost, high efficiency, simple operation, etc., which attracts more and more researchers' attention [5]. The current research focuses on developing highly efficient and easily renewable adsorption materials for treating printing and dyeing wastewater.

It is well known that adsorbent selection plays a vital role in adsorption. In recent years, hydrogel, functional material with hydrophilic groups and strong adsorption capacity, has shown great potential in water treatment [6]. Hydrogel is a high molecular polymer that can absorb much water without being dissolved in water. There are many active functional groups on the three-dimensional network structure of the polymer backbone. Due to the advantages of a wide source of raw materials, low cost, good biocompatibility, and excellent dye binding ability, many researchers have used natural polysaccharide polymers such as sodium alginate (SA), sodium carboxymethyl cellulose, and starch in the development of hydrogels [7]. However, traditional hydrogels are limited by their material and structural characteristics, with slow adsorption rate, lack of strong adsorption capacity, chemical and thermal stability, mechanical strength, and high recycling rate, which leads to their inability to be widely used in actual water treatment [8]. Thus, preparing a hydrogel with a rapid adsorption rate, strong adsorption performance, and high mechanical strength is significant for its practical application.

As a biodegradable natural sodium salt, SA has the characteristics of a sustainable biomaterial matrix. The hydrogel's adsorption performance can be enhanced by the synergistic effects between the carboxyl functional groups widely distributed on the molecular backbone of SA and the active functional groups on the polymer molecular chains [9]. Graphene oxide (GO) is a high specific surface area nanomaterial rich in hydroxyl, carboxyl, epoxy, and other oxygen-containing functional groups. It performs excellently in wastewater treatment and purification and is a highly efficient adsorption material [10]. Due to the excellent dispersion and nano-size characteristics of GO in water, it is not easy to separate from pollutants after adsorption. In practical applications, GO is often separated and reused by chemical modification or by composites with other materials. The oxygen-containing functional groups on the GO surface can form an excellent interfacial interaction with the hydrogel through chemical or hydrogen bonding. It is helpful to design a highly adsorbable hydrogel with effectively improved mechanical properties and adsorption characteristics. In addition, introducing a porous structure through the hydrogel is conducive to the entry and exit of dye molecules and can also enhance the response of the hydrogel to external stimuli. Therefore,

this hydrogel with robust mechanical properties, high adsorption performance, and a fast response rate has a good application prospect as an adsorption material.

Based on the above strategy, we prepared a high-performance hydrogel using a simple one-pot method in this work. The introduction of GO into the hydrogel matrix can not only enhance the toughness of the hydrogel but also significantly enhance its mechanical properties. In the polymerization process, bubbles were introduced into the hydrogel precursor by stirring foaming, the surfactant sodium dodecyl sulfate was added to stabilize the bubbles, and SA was introduced to regulate the rheological properties to promote stability. The structure and properties of hydrogels were thoroughly tested, and the adsorption thermodynamics, kinetics, and mechanism of the hydrogels were analyzed. The novel hydrogel we designed can be used as an effective adsorbent for treating of printing and dyeing wastewater.

Materials and methods

Materials

Acrylic acid (AA, 99%), 2-acrylamido-2-methyl-1-propane sulfonic acid (AMPS, 98%), sodium alginate (SA, chemically pure), N, N-methylenebisacrylamide (NMBA, 99%), ammonium persulfate (APS, 98%), sodium dodecyl sulfate (SDS, 98%), sodium hydroxide (96%), graphene oxide (GO, 99%), sodium chloride (99%), potassium chloride (99%), calcium chloride (98%), aluminum chloride (99%), methylene blue (MB, 98%), and hydrochloric acid (36.5%) were purchased from Sinopharm Chemical Reagent Co., Ltd, China. Deionized water, tap water, lake water (Qingfeng Lake, Dongying, China), and river water (Guangli River, Dongying, China) were used for the experiments.

Preparation of graphene oxide/sodium alginate composite hydrogel

Take one of the polymerization reactions as an example: 21.60 g AA was neutralized with 40% NaOH solution (9.60 g NaOH dissolved in 14.40 ml distilled water) under an ice-water bath. Then, 4.32 g AMPS, 0.1728 g GO, 0.25 g APS, 0.04 g NMBA, 0.20 g SDS, and the dissolved SA solution (2.00 g SA dissolved in 100 ml distilled water) were added to the above solution. The mixture was ultrasonically dispersed for 30 min at room temperature. The whole system was then kept at 65 ℃ for 4 h. After the hydrogel formed, the product was washed several times with deionized water. The prepared composite hydrogel was dried in a vacuum oven at 75 ℃. Finally, the product was obtained after crushing and milling through a 30–50 mesh screen. The polymerization mechanism for the preparation of composite hydrogels is shown in Fig. 1.

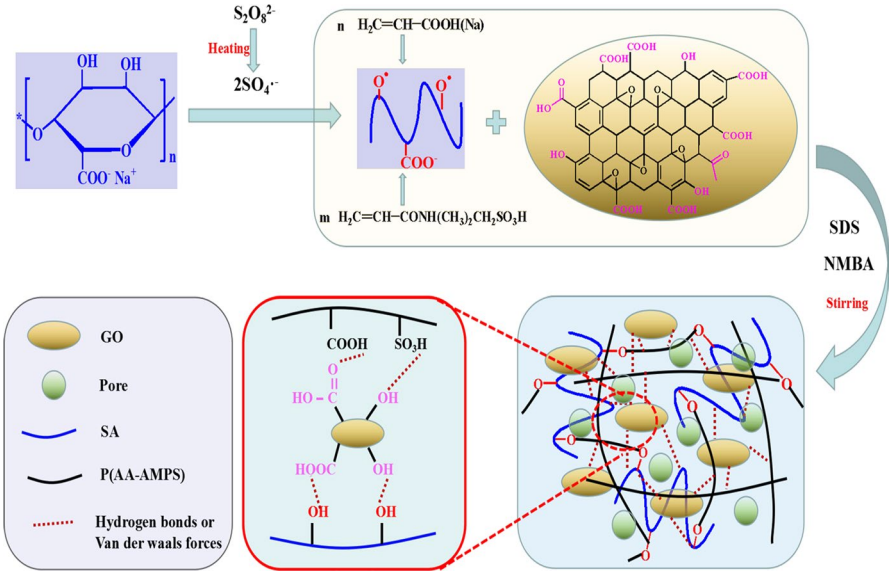

Fig. 1 Preparation mechanism of the composite hydrogel

Determination of hydrogel properties

Swelling property

The hydrogel samples were immersed in sufficient solution to reach swelling equilibrium at room temperature. The swollen samples were then separated from the unabsorbed water using 100 sieve targets. The swelling ratio of the hydrogel is calculated as follows (Eq. (1)) [11]:

$$\mathrm{SR} = (M_2 - M_1)/M_1 \tag{1}$$

where, M_1 is the mass of the dry hydrogel, and M_2 is the mass of the hydrogel after water absorption.

Adsorption property

100 mg of dried hydrogel sample was added to the 100 mL MB solution, and then the above system was oscillated and adsorbed for 90 min. The effects of GO dosage, initial MB concentration, pH, temperature, co-existing ions, and water quality on adsorption capacity were extensively investigated. The concentration of MB in the adsorbed solution was determined by the standard spectrophotometric method. To ensure the accuracy of data processing, all the adsorption tests were performed at least three times. The removal efficiency (R, %) (Eq. (2)) and the adsorption capacity (Q, mg/g) (Eq. (3)) were calculated using the following formula [12]:

$$R(\%) = \frac{C_0 - C_e}{C_0} \times 100 \tag{2}$$

$$Q = \frac{C_0 - C_e}{m} \times V \tag{3}$$

where C_0 and C_e are the initial and equilibrium MB concentration, mg/L; m is the mass of the dried hydrogel, g; V is the volume of the MB solution, L.

Mechanical property

The tensile properties of the hydrogel were tested using a CMT4102 universal testing machine at room temperature. The sample used for the tensile test is 5 mm in diameter, 30 mm in length, and a tensile rate of 50 mm/min. To ensure the same water content of hydrogels tested for mechanical properties, the hydrogels should be dried before swelling. After dialysis and freeze-drying, the hydrogels should be properly swollen in distilled water to control the water content of the hydrogels at about 10%.

Reusability property

The composite hydrogels after adsorption were collected and dried at 75 ℃, and then desorbed and regenerated 8 times with 0.2 mol/L HCl solution [13].

Structural characterization

The analysis of structural characteristics was carried out by NICOLETIN10 spectrometer (Thermo Fisher Scientific, USA), FEI QUANTA FEG450 scanning electron microscope (Fei Company, USA), OLS5000-SFA (Olympus, Japan) confocal laser scanning microscope, and nitrogen adsorption instrument, AutoSorbiQ2 (Quantachrome, USA). NMR spectra were recorded on a Bruker AVIII spectrometer (Germany, ^{13}C frequency of 125.13 MHz).

Results and discussion

Characterization and BET analysis

It is well known that the porous structure is favorable for the adsorption of dyes by hydrogels. It can be seen from Fig. 2a and b that P(AA-AMPS)/SA-GO shows a prominent three-dimensional network structure, a typical honeycomb structure with interconnected pores. The highest altitude of the hydrogel is 570 μm in the map of the altitude distribution over an area of about 800 μm × 600 μm. Furthermore, N_2 adsorption is performed on the composite hydrogel to evaluate the porosity. As shown in Fig. 2c and f, the composite hydrogels exhibit a reversible type IV isotherm and H3 hysteresis

Fig. 2 **a** 3D microscopic topography of P(AA-AMPS)/SA-GO **b** SEM image of P(AA-AMPS)/SA-GO **c** ▶ nitrogen adsorption–desorption isotherm curves **d** Rouquerol transformation diagram of adsorption data **e** linear fitting diagram of adsorption data after BET transformation **f** pore width distributions of the hydrogel **g** FTIR spectra of samples **h** ^{13}C-NMR spectrum of P(AA-AMPS)/SA-GO as obtained by solid-state NMR

loop, one of the mesoporous materials' main characteristics. The N_2 adsorption capacity of P(AA-AMPS)/SA-GO with SDS is higher than that of the hydrogel without SDS. The BET surface area and the pore size of P(AA-AMPS)/SA-GO with SDS are 160.3 $m^2 \cdot g^{-1}$ and 9.2 nm, respectively. The composite hydrogel contains many mesoporous pores, and the peak pore size is about 10 nm. Strictly speaking, the BET evaluation of mesoporous samples has certain limitations. Therefore, Rouquerol transformation is performed on the adsorption data. As shown in Fig. 2d, the maximum allowable relative pressure is 0.36 for hydrogel with SDS and 0.27 for hydrogel without SDS. The BET equation is used for the linear fitting of Rouquerol plots, and the results are shown in Fig. 2e. The data points after Rouquerol transformation increase monotonically with the increase in p/p_0, indicating that the adsorption process conforms to the BET model. Moreover, the BET constants [V_m (the amount of monolayer gas adsorbed per unit mass of sample) and C (the constant associated with the heat of adsorption)] are obtained based on the linear fitting equation (Table 1). The above analysis shows that the composite hydrogel has abundant pore structure and high specific surface area, which undoubtedly promotes its adsorption performance.

The FTIR spectra of GO, SA, and P(AA-AMPS)/SA-GO are displayed in Fig. 2g. In the curve of GO, the peak at 3247 cm^{-1} is the stretching vibration peak of –OH, the band at 1589 cm^{-1} is the stretching vibration peak of C=C, the peak near 1411 cm^{-1} belongs to the bending vibration peak of –OH, and 1023 cm^{-1} is the stretching vibration absorption peak of C–O of the epoxy group. These peaks prove that the GO surface contains functional groups such as epoxy and hydroxyl. The peaks at 3386 and 1620 cm^{-1} in the spectrum of SA are attributed to the stretching vibration of –OH and –C=O, respectively [14]. The peaks of unsaturated C-H disappear after polymerization, and the absorption peaks corresponding to GO and SA can almost be found in the product spectra, indicating that P(AA-AMPS)/SA-GO is prepared successfully. Figure 2h shows the solid state ^{13}C NMR spectrum of the hydrogel. The ^{13}C NMR spectrum is obviously divided into three parts. Broad ^{13}C resonances between 50 and 110 ppm are mainly assigned to the carbons of SA. Resonances at 40.4 and 45.9 ppm are assigned to the carbons of $–CH_2–CH–$ in the polymer chains. Resonances around 184.9 ppm are attributed to the carbons of –COOH(Na), –CONH groups inside the hydrogel. In addition, the resonance of –C=C– cannot be observed in the spectrum, indicating that AA and AMPS are successfully grafted onto SA.

Effect of GO dosage on mechanics, water absorption, and adsorption properties of hydrogels

Tensile stress–strain curves of P(AA-AMPS)/SA-GO composite hydrogels with different GO contents are shown in Fig. 3a. As the GO content increases, the tensile strength and elongation at the break of the composite hydrogel also increase.

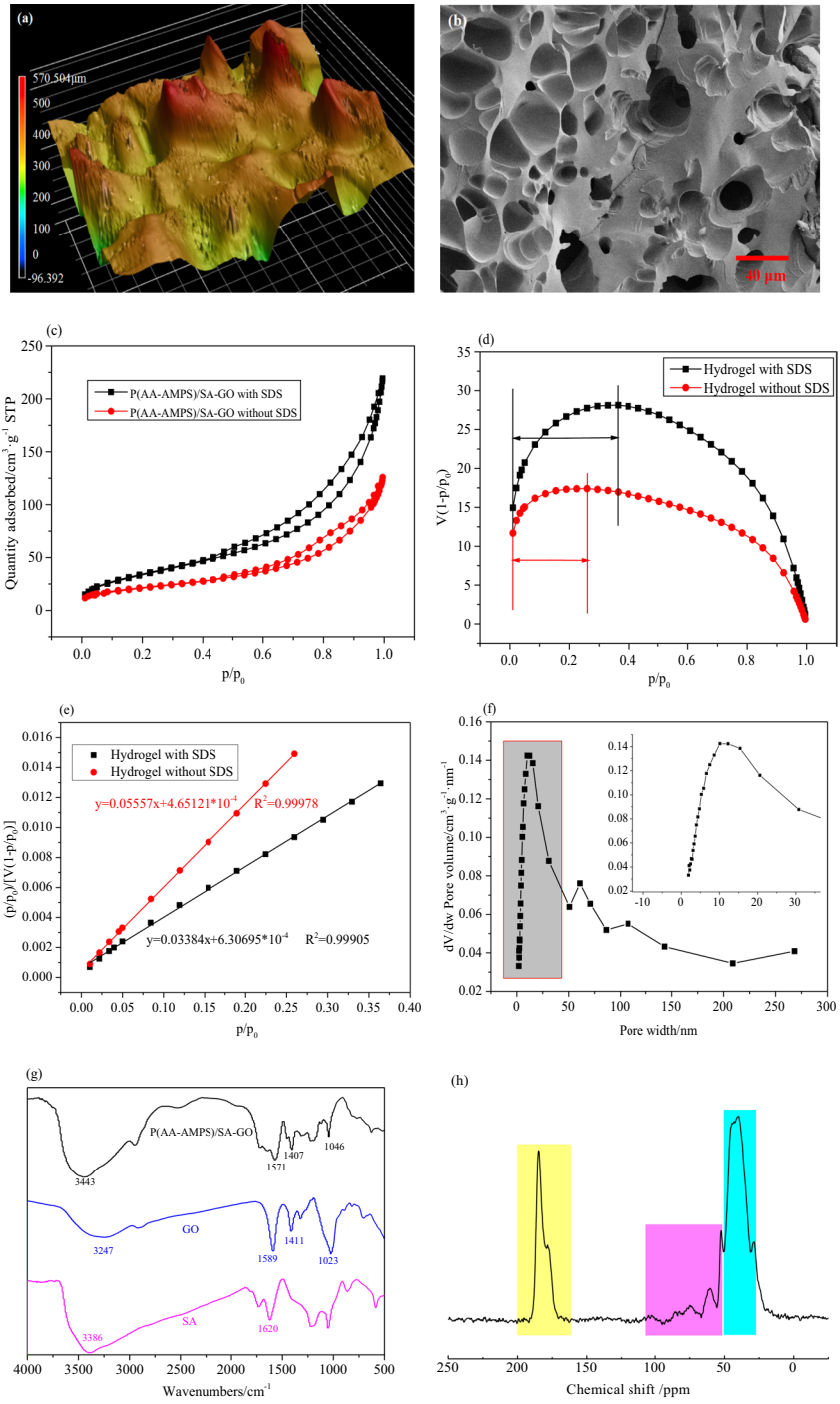
(a)
570.504μm
500
400
300
200
100
0
-96.392
(b)
40 μm
(c)
P(AA-AMPS)/SA-GO with SDS
P(AA-AMPS)/SA-GO without SDS
Quantity adsorbed/cm³·g⁻¹ STP
p/p0
(d)
Hydrogel with SDS
Hydrogel without SDS
V/(1-p/p0)
p/p0
(e)
Hydrogel with SDS
Hydrogel without SDS
y=0.05557x+4.65121*10⁻⁴ R²=0.99978
y=0.03384x+6.30695*10⁻⁴ R²=0.99905
(p/p0)/[V(1-p/p0)]
p/p0
(f)
dV/dw Pore volume/cm³·g⁻¹·nm⁻¹
Pore width/nm
(g)
P(AA-AMPS)/SA-GO
3443
1571
1407
1046
GO
3247
1589
1411
1023
SA
3386
1620
Wavenumbers/cm⁻¹
(h)
Chemical shift /ppm

Table 1 BET constants based on Rouquerol plots

	C	V_m ($cm^3 \cdot g^{-1}$)	S_{cal} ($m^2 \cdot g^{-1}$)	S_{exp} ($m^2 \cdot g^{-1}$)
Hydrogel with SDS	54.7	29.0	126.3	160.3
Hydrogel without SDS	120.5	17.9	77.7	125.8

The addition of GO increases the number of hydrogen bonds in the crosslinked network of the composite hydrogel, leading to an increase in the degree of network cross-linking of P(AA-AMPS)/SA-GO. The enhanced physical crosslinking increases the tensile strength of the composite hydrogel and also increases the flexibility of the macromolecular chain so that the composite hydrogel eventually breaks with a significant elongation at break. This shows that the tensile strength, elongation at break, and mechanical properties of the P(AA-AMPS)/SA-GO composite hydrogel are significantly improved by the addition of GO. However, when the GO content is higher than 0.8%, the strain of the composite hydrogel decreases significantly, and the tensile strength increases significantly. This is because the increase in GO makes the total amount of crosslinking agents in the hybrid system more extensive, which increases the crosslinking density between polymer segments and restricts the movement of polymer segments. At this point,

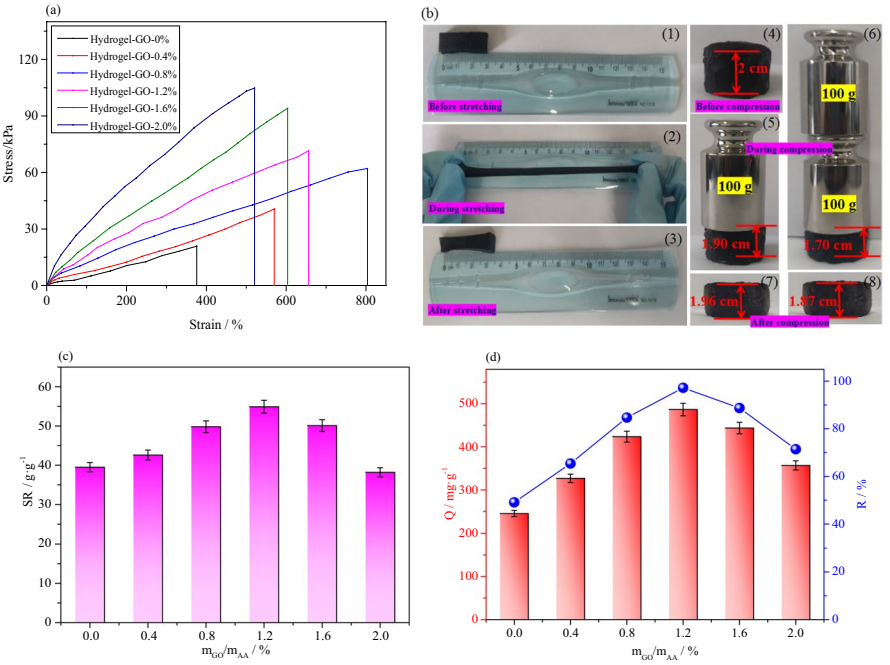

Fig. 3 **a** Tensile stress–strain curves of hydrogels **b** photograph of the mechanical properties of hydrogel **c** effect of GO dosage on swelling property **d** effect of GO dosage on MB adsorption

GO has a greater reinforcing strengthening effect on the crosslinking density, so the tensile strength of the hydrogel increases at a similar strain. However, if the crosslinking density is too high, the polymer chain segment of the hydrogel will be easily damaged and unable to recover its original shape after being subjected to a larger external force, thus reducing the elongation at break of the hydrogel. When the GO content is 0.8% and 2.0%, respectively, the maximum elongation at break and tensile strength can reach 803% and 104.8 kPa, respectively. It can be seen from Fig. 3b that the composite hydrogel can be significantly elongated under tension. After removing the external force, the composite hydrogel can essentially recover to its original length with no apparent damage. When the composite hydrogel is compressed by pressure, it can produce some deformation, but there is no noticeable damage. The above experimental phenomenon shows that P(AA-AMPS)/SA-GO composite hydrogel has good elastic deformation, mechanical strength, and self-recovery characteristics.

The influence of GO dosage on the swelling and adsorption properties of P (AA-AMPS)/SA-GO is shown in Fig. 3c and d. As the GO dosage increases, the swelling ratio and the adsorption capacity first increase and then decrease. When the GO dosage is 1.2%, the swelling ratio and MB adsorption are the highest, 54.9 g/g and 486.5 mg/g, respectively. This is because the hydrophilic oxygen-containing active groups on the GO surface can combine with the –COOH, –OH groups on the polymer chains to form a more stable network structure, thus increasing the specific surface area of the gel network, enabling it to absorb more water and MB molecules (The surface areas of hydrogels with GO dosages of 0, 0.4, 0.8, 1.2, 1.6, 2.0% are 97.3, 123.6, 136.8, 160.3, 153.6, 130.5 m^2/g, respectively.). The non-crosslinked hydrophilic groups in GO can bind with the water and MB molecules, increasing the adsorption capacity of the hydrogel. As the concentration of GO is further increased, the internal crosslinking density of the hydrogel increases, reducing the adsorption network space and its adsorption capacity. Considering its adsorption performance and mechanical strength, we choose the optimal dosage of GO as 1.2%.

Swelling property of P(AA-AMPS)/SA-GO

The swelling property of gel materials is an essential factor in the adsorption process. Figure 4 describes the influence of different water sources and pH values on the swelling characteristics of the composite hydrogel. It can be seen that the swelling ratio in distilled water is higher than that in other waters. This phenomenon may be because the co-existing ions will reduce the osmotic pressure between the external environment and the hydrogel, resulting in a gradual decrease in water absorption. It is also found that pH significantly affects the swelling ratio of the hydrogel. As the pH increases, the swelling ratios increase and then decrease. At a pH of 8, the maximum water absorption rate is 54 g/g. This is because the protonation of carboxyl and sulfonic groups in an acid solution and the charge shielding effect in alkaline conditions weakens the electrostatic repulsion in the gel, resulting in the gel's inability to stretch and swell fully [15].

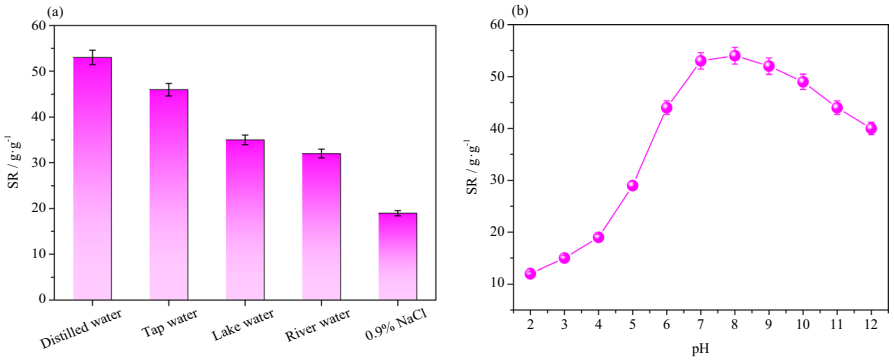

Fig. 4 **a** Swelling properties of hydrogel in different water bodies **b** effect of pH on water absorption of hydrogel

Adsorption performance of P(AA-AMPS)/SA-GO

Influence of external factors on adsorption properties of hydrogel

To measure the practical application performance of the hydrogel, we comprehensively investigate the influence of the water environment on the adsorption performance, and the results are shown in Fig. 5.

The effect of the amount of hydrogel on the adsorption performance was investigated at the initial MB mass concentration of 500 mg/L. As shown in Fig. 5a, the adsorption capacity gradually decreases, and the MB removal rate gradually increases with increasing the amount of hydrogel. When the amount of hydrogel increases, the adsorption sites provided by the excess hydrogel have reached saturation in the solution, and the adsorption process reaches equilibrium. The excess hydrogel does not participate in the adsorption process of MB. When the hydrogel dosage is 0.01 g, the adsorption capacity is the highest, up to 680 mg/g; when the hydrogel is 0.1 g, the dye removal rate is 97.2%, and the adsorption is complete.

The effect of the initial mass concentration of MB on the adsorption performance at room temperature was investigated, and the results are shown in Fig. 5b. It can be seen that as the MB concentration increases, the adsorption capacity first increases and then reaches adsorption equilibrium. This is because, with the rise in the MB concentration, the contact opportunities between MB and the hydrogel surface increase significantly. The active adsorption sites are utilized, which favors the adsorption process. When the adsorption sites are fully occupied, the adsorption reaches equilibrium, and the adsorption capacity does not increase after that. The maximum adsorption capacity reaches 689.9 mg/g at the MB concentration of 1300 mg/g.

The pH of the solution affects the structure of dye molecules and the charge characteristics of the adsorbent surface. It can be seen from Fig. 5c that as the pH increases from 2 to 5, the adsorption capacity for MB increases rapidly from 89.8 to 365.9 mg/g. When the pH exceeds 5, the amount of MB adsorbed on the

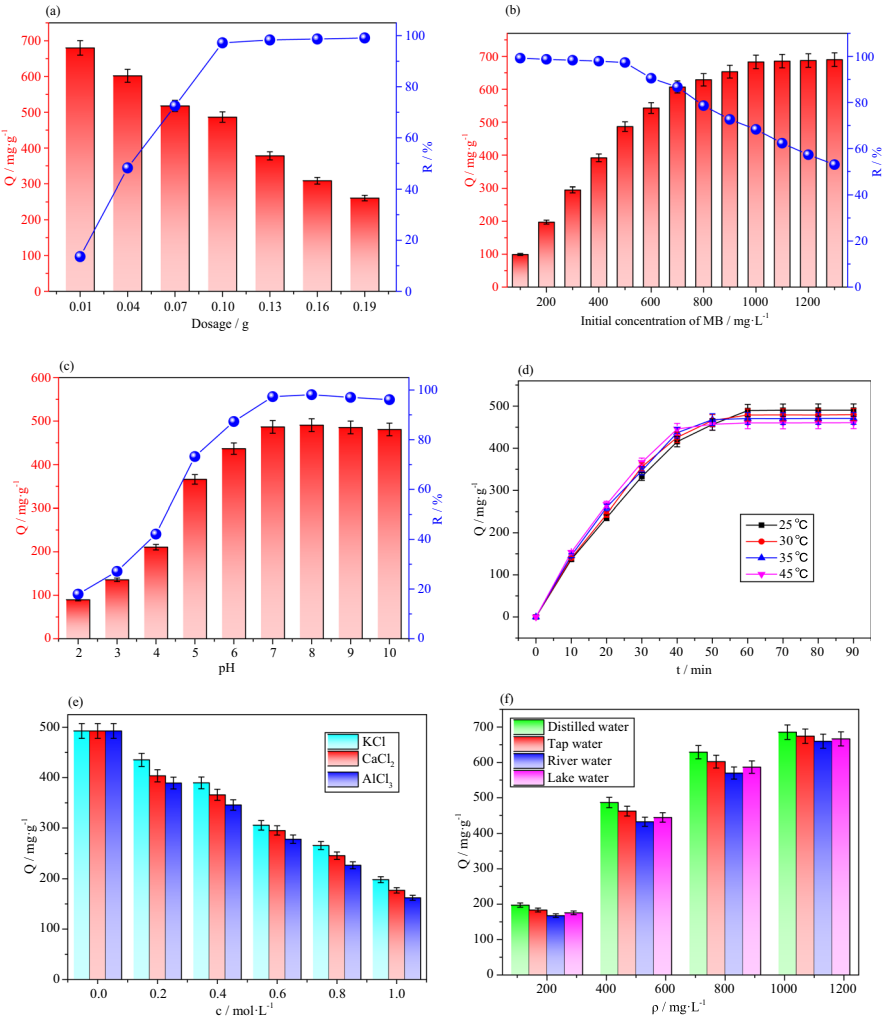

Fig. 5 Influence of external factors on adsorption properties of hydrogel **a** hydrogel dosage **b** MB initial concentration **c** pH **d** adsorption time and temperature **e** coexisting ions **f** water quality

hydrogel remains at a high level, and the highest adsorption capacity occurs at pH = 8, 490.5 mg/g. At low pH, the carboxyl, sulfonic, and hydroxyl groups on the hydrogel are easily protonated by the excess H^+. These groups repel each other with the MB cation. In addition, hydrogen bonds are easily formed between the groups in the hydrogel, leading to network contraction and hindering the diffusion of MB molecules. As the pH increases, the degree of protonation decreases. The electrostatic attraction between the MB cation and negatively charged groups increases, and the adsorption capacity gradually increases [16].

Figure 5d shows the influence of adsorption time and temperature on the adsorption performance of the hydrogel. It can be seen that the hydrogel can reach the

adsorption equilibrium within 60 min. Such rapid adsorption kinetics is mainly due to the porous structure and abundant adsorption sites on the surface of the hydrogel. In addition, the higher the temperature is, the shorter the time required for the hydrogel to reach the adsorption equilibrium. However, the adsorption amount decreases, indicating that the adsorption process is exothermic.

Figure 5e shows the effect of co-existing ions on adsorption capacity. The results show that the adsorption capacity of the hydrogel for MB decreases as the ionic strength increases. The adsorption of MB is obviously inhibited when the ionic strength is high. The increase in ionic strength enhances the interaction force between ions and prevents the diffusion of MB from the solution to the surface of the hydrogel. The order in which coexisting cations affect the adsorption of MB by the hydrogel is $Al^{3+} > Ca^{2+} > K^{+}$. MB is a cationic dye, and coexisting cations have competitive adsorption with MB. The above phenomena also reveal that the adsorption process is controlled by ion exchange.

The dye removal performance of the hydrogel in different water bodies is shown in Fig. 5f. Various water bodies have different effects on the dye adsorption properties of hydrogels. The adsorption capacity of MB in deionized water is higher than that in other water bodies, indicating that co-existing ions in different water bodies can form competitive adsorption with MB. This also teaches us a lesson: in practice, we must clearly understand water quality.

Adsorption isotherms

To determine the type of adsorption isotherm, Langmuir (Eq. (4)) and Freundlich's (Eq. (5)) models are used to fit the data linearly, and the results are shown in Fig. 6 [17]. At 25 ℃, the fitting correlation coefficients R^2 of the Langmuir and Freundlich adsorption isotherms of hydrogel on MB are 0.9664 and 0.8363, respectively, indicating that the Langmuir model can better describe the adsorption process of the hydrogel. Therefore, the adsorption of MB on the hydrogel is monolayer adsorption, and most of the MB molecules are adsorbed on the active sites on the surface of the composite hydrogel.

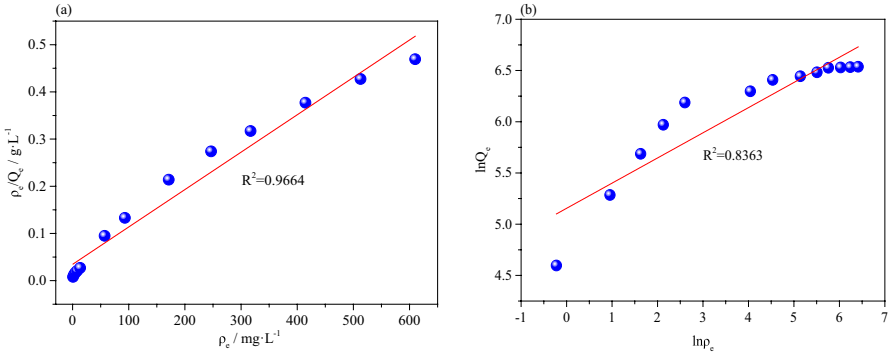

Fig. 6 Adsorption isotherms of **a** Langmuir model **b** Freundlich model

$$\frac{\rho_e}{Q_e} = \frac{1}{Q_0 K_b} + \frac{\rho_e}{Q_0} \tag{4}$$

$$\ln Q_e = \ln K_f + \frac{1}{n}\ln \rho_e \tag{5}$$

where ρ_e is the MB concentration after adsorption, mg/L; Q_e is the equilibrium adsorption capacity, mg/g; Q_0 is the maximum theoretical adsorption capacity, mg/g; K_b is the adsorption constant, L/mg; K_f is the adsorption constant, $mg^{1-n}{\cdot}L^n{\cdot}g^{-1}$; n is the adsorption index.

Adsorption kinetics

The adsorption kinetics of MB by hydrogel is shown in Fig. 7. The pseudo-first-order model (Eq. (6)), pseudo-second-order model (Eq. (7)), and intra-particle diffusion model (Eq. (8) are used to fitting the data [18].

$$\log(Q_e - Q_t) = -\frac{k_1}{2.303}t + \log Q_e \tag{6}$$

$$\frac{t}{Q_t} = \frac{t}{Q_e} + \frac{1}{k_2}\frac{1}{Q_e^2} \tag{7}$$

$$Q_t = k_i t^{\frac{1}{2}} + M \tag{8}$$

where M is the parameter related to the thickness of the interface layer; k_i is the diffusion constant, $mg/(g{\cdot}min^{1/2})$; Q_t is the adsorption capacity of the composite hydrogel to MB at time t, mg/g; t is the adsorption time, min; Q_e is the equilibrium adsorption capacity, mg/g; k_1 and k_2 are pseudo-first and pseudo-second-order adsorption rate constants, respectively.

The whole adsorption process can be divided into two stages. At the initial stage, the adsorption rate is fast. After one hour of adsorption, hydrogel's adsorption capacity on MB exceeded 90% of the equilibrium adsorption capacity. As the time increases, the adsorption rate gradually decreases and reaches equilibrium after 1.5 h. This may be due to the presence of many active sites on the surface of the hydrogel at the initial stage. The ion concentration difference between the liquid and solid surfaces is significant, which makes it easy for MB to diffuse quickly to the surface of the hydrogel sphere for reaction, so the adsorption rate is fast. With the process of adsorption, the active sites on the surface of hydrogel that can bind with MB gradually decrease, reducing the adsorption rate until equilibrium is reached.

As can be seen from Fig. 7a and b, the pseudo-second-order kinetic model is more suitable for the adsorption process of the hydrogel compared to the pseudo-first-order kinetic model, indicating that chemisorption exists in the adsorption process of MB. Although the pseudo-second-order model fits the experimental data well, more is needed to explain the diffusion mechanism. Therefore, the in-particle

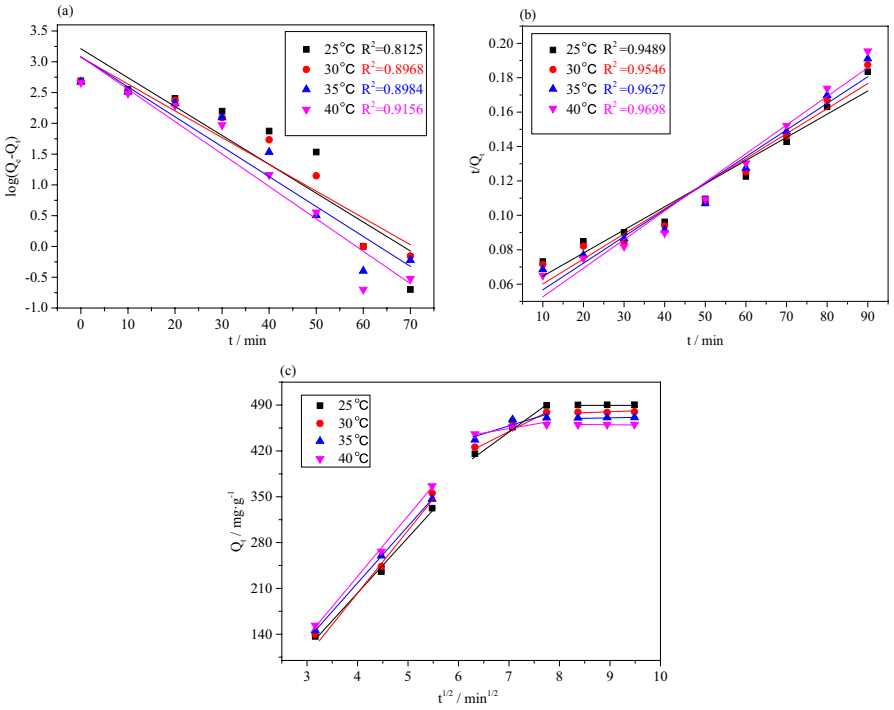

Fig. 7 Fitting curves of pseudo-first-order **a** and pseudo-second-order **b** models and intraparticle diffusion model **c**

diffusion model is used to further investigate the control steps of the adsorption rate and diffusion mechanism. As shown in Fig. 7c, the adsorption of MB by the composite hydrogel is a multistep adsorption process. In the first stage, the adsorption amount of MB is high, due to the rapid diffusion of MB on the surface of the hydrogel. In the second stage, the adsorption rate becomes slow, and the adsorption occurs in tiny pores. At this stage, the internal diffusion of the particles is a major limiting factor. In the third stage, the concentration of MB in the solution and the reactive active sites in the hydrogel are very low, and the adsorption is close to equilibrium. Since the curve does not pass through the origin, it shows that particle diffusion is not the only factor controlling the rate. It can be inferred that particle and membrane diffusion occur together in adsorption.

Adsorption thermodynamics

To study the thermodynamic properties of MB adsorption by hydrogel, the free energy change (ΔG), enthalpy change (ΔH), and entropy change (ΔS) are calculated, and the calculation formulas were respectively shown in Eqs. (9, 10), respectively [18]. The van't Hoff curve and thermodynamic parameters are displayed in Fig. 8 and Table 2, respectively. $\Delta G < 0$ at different temperatures indicates that the adsorption process is spontaneous. $\Delta H < 0$ suggests that the adsorption process is

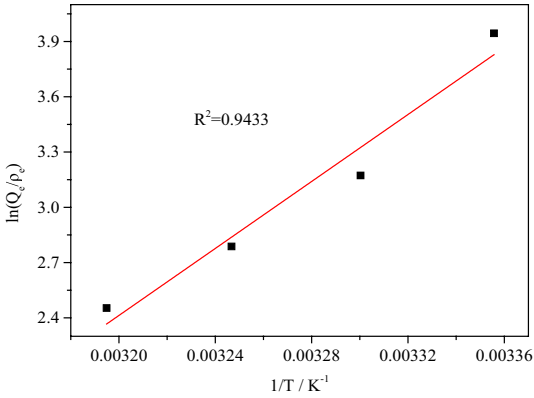

Fig. 8 Van't Hoff curve

Table 2 Thermodynamic parameters

T (K)				*ΔH* (kJ/mol)	*ΔS* (J/mol·K)
298	303	308	313		
Δ*G*(kJ/mol)					
− 9.49	− 8.39	− 7.28	− 6.17	− 75.55	− 221.65

exothermic, and increasing the temperature is not conducive to the adsorption of MB. $\Delta S < 0$ means that the confusion of the MB adsorption process decreases. In addition, the $|\Delta H|$ of the physical adsorption is generally in the range 0 ~ 20 kJ/mol, and the $|\Delta H|$ of the chemical adsorption is more than 20 kJ/mol. In this experiment, the $|\Delta H|$ is 75.55 kJ/mol, further confirming that the adsorption behavior of MB is mainly chemical adsorption.

$$\ln\frac{Q_e}{\rho_e} = \frac{\Delta S}{R} - \frac{\Delta H}{RT} \tag{9}$$

$$\Delta G = \Delta H - T\Delta S \tag{10}$$

where ρ_e is the MB concentration after adsorption, mg/L; Q_e is the equilibrium adsorption capacity, mg/g.

Reuse performance

Recyclability is an essential factor in evaluating the performance of adsorbent. The adsorbed hydrogel was desorbed in a hydrochloric acid solution, and then the adsorption experiment was repeated. The results show that the composite hydrogel

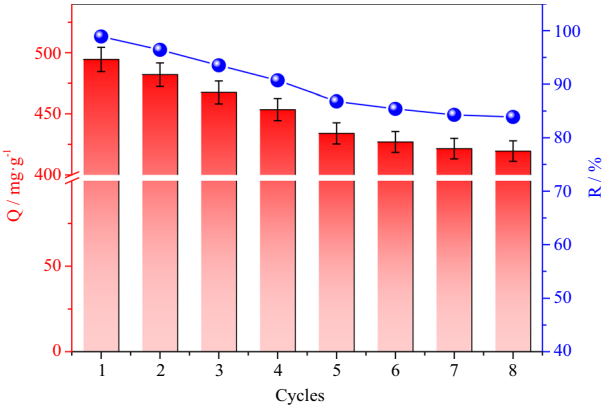

Fig. 9 Reusability of P(AA-AMPS)/SA-GO hydrogel for the adsorption of MB

has good regeneration and adsorption properties and can be reused. After eight consecutive adsorption–desorption cycles, the adsorption capacity could reach 419.5 mg/g (Fig. 9). As the number of cycles increased, the adsorption amount decreased slightly, possibly due to the incomplete elution of methylene blue adsorbed in the last cycle.

Finally, we compare the differences in MB removal between the composite hydrogels prepared in this study and those reported in other literature. As displayed in Table 3, P(AA-AMPS)/SA-GO shows better MB removal performance, especially regarding adsorption rate and reusability. Therefore, P(AA-AMPS)/SA-GO hydrogel has broad application prospects in dyeing wastewater treatment.

Conclusion

A kind of adsorption hydrogel P(AA-AMPS)/SA-GO with good mechanical properties and a fast adsorption rate was prepared by a simple one-pot method. The hydrogel was characterized and analyzed by SEM, FT-IR, CLSM, and BET. The results showed that the hydrogel was successfully prepared. The mechanical properties of the composite hydrogel can be adjusted by changing the amount of GO in the composite hydrogel. The maximum absorption at break and tensile strength can reach 803% and 104.8 kPa, respectively. The composite hydrogel shows rapid and high-capacity adsorption of cationic dye MB. In 500 mg/L MB solution, the highest MB removal rate is 98.1% in 90 min. The MB removal rate of the composite hydrogel was still higher than 80% after eight adsorption–desorption cycles. The composite hydrogel with high strength, high dye adsorption capacity, and reusability has good application prospects in the treatment of cationic dye wastewater.

Table 3 Comparison of the absorption capacity of P(AA-AMPS)/SA-GO and other hydrogel composites on MB

Adsorbents	Equilibrium adsorption capacity of MB (mg/g)	Time required to reach adsorption equilibrium (min)	Number of cycles and removal efficiency	References
SA-CH	328.6	300	6, 97.0%	[19]
Agar/κ-carrageenan hydrogel	242.3	2800	5, 52.8%	[20]
O-CM-chitosan hydrogel	434.8	3500	4, 48.0%	[21]
CS50 hydrogel	2000	600	4, 50.0%	[22]
Poly (acrylic acid)/chitosan-g-polyvinylamine composite hydrogel	596.2	1800	5, 85.0%	[23]
Apatite/Attapulgite/Alginate composite hydrogel	256.0	300	–	[24]
P(AA-AMPS)/SA-GO	689.9	90	8, 83.9%	Current research

Authors' contributions XW, contributed to the conception of the study; YZ, performed the experiment and wrote the manuscript; LZ, performed the data analyses.

Funding This work was supported by the Dongying scientific development fund (DJ2021021) (DJ2021018).

Data availability All data generated or analyzed during this study are included in this published article.

Code availability Not applicable.

Declarations

Conflicts of interest The authors declare there is no conflicts of interest regarding the publication of this paper.

Ethical approval Not applicable.

Consent to participate Not applicable.

Consent for publication The paper has not been published elsewhere, and it has not been submitted simultaneously for publication elsewhere. The authors agree to publication in the journal.

References

1. Crini G, Lichtfouse E (2019) Advantages and disadvantages of techniques used for wastewater treatment. Environ Chem Lett 17:145–155. https://doi.org/10.1007/s10311-018-0785-9
2. Mohsenpour SF, Hennige S, Willoughby N, Adeloye A, Gutierrez T (2021) Integrating micro-algae into wastewater treatment: a review. Sci Total Environ 752:142168. https://doi.org/10.1016/j.scitotenv.2020.142168
3. Rashid R, Shafiq I, Akhter P, Iqbal MJ, Hussain M (2021) A state-of-the-art review on wastewater treatment techniques: the effectiveness of adsorption method. Environ Sci Pollut Res 28:9050–9066. https://doi.org/10.1007/s11356-021-12395-x
4. Chai WS, Cheun JY, Kumar PS, Mubashir M, Majeed Z, Banat F, Show PL (2021) A review on conventional and novel materials towards heavy metal adsorption in wastewater treatment application. J Clean Prod 296:126589. https://doi.org/10.1016/j.jclepro.2021.126589
5. Velusamy S, Roy A, Sundaram S, Kumar Mallick T (2021) A review on heavy metal ions and containing dyes removal through graphene oxide-based adsorption strategies for textile wastewater treatment. Chem Rec 21:1570–1610. https://doi.org/10.1002/tcr.202000153
6. Yang J, Chen X, Zhang J, Wang Y, Wen H, Xie J (2021) Role of chitosan-based hydrogels in pollutants adsorption and freshwater harvesting: a critical review. Int J Biol Macromol 189:53–64. https://doi.org/10.1016/j.ijbiomac.2021.08.047
7. Han D, Zhao H, Gao L, Qin Z, Ma J, Han Y, Jiao T (2021) Preparation of carboxymethyl chitosan/phytic acid composite hydrogels for rapid dye adsorption in wastewater treatment. Colloids Surf A Physicochem Eng Asp 628:127355. https://doi.org/10.1016/j.colsurfa.2021.127355
8. Lü T, Ma R, Ke K, Zhang D, Qi D, Zhao H (2021) Synthesis of gallic acid functionalized magnetic hydrogel beads for enhanced synergistic reduction and adsorption of aqueous chromium. Chem Eng J 408:127327. https://doi.org/10.1016/j.colsurfa.2021.127355
9. Xie M, Zeng Y, Wu H, Wang S, Zhao J (2022) Multifunctional carboxymethyl chitosan/oxidized dextran/sodium alginate hydrogels as dressing for hemostasis and closure of infected wounds. Int J Biol Macromol 219:1337–1350. https://doi.org/10.1016/j.ijbiomac.2022.08.166

10. Yi J, Choe G, Park J, Lee JY (2020) Graphene oxide-incorporated hydrogels for biomedical applications. Polym J 52:823–837. https://doi.org/10.1038/s41428-020-0350-9
11. Srikaew M, Jumpapaeng P, Suwanakood P, Kaiyasuan C, Promarak V, Saengsuwan S (2023) Rapid synthesis and optimization of UV-photopolymerized cassava starch-based superabsorbent hydrogels as a biodegradable, low-cost, and effective adsorbent for MB removal. J Ind Eng Chem 118:53–69. https://doi.org/10.1016/j.jiec.2022.10.045
12. Patra BR, Nanda S, Dalai AK, Meda V (2021) Taguchi-based process optimization for activation of agro-food waste biochar and performance test for dye adsorption. Chemosphere 285:131531. https://doi.org/10.1016/j.chemosphere.2021.131531
13. Wang X, Zheng Y, Zong L, Zhang C, Ren X, Ding Y, Zhou Y (2022) Porous biochar composite hydrogel for effective removal of low-concentration methylene blue from wastewater. J Polym Res 29:1–15. https://doi.org/10.1007/s10965-022-03295-w
14. Zhu L, Liu Y, Wang F, He T, Tang Y, Yang J (2018) Preparation and the swelling properties of sodium alginate graft poly (acrylic acid-co-2-acrylamide-2-methyl propane sulfonic acid)/graphene oxide hydrogel composite. Adv Polym Technol 37:2885–2893. https://doi.org/10.1002/adv.21960
15. Meng Y, Ye L (2017) Synthesis and swelling property of superabsorbent starch grafted with acrylic acid/2-acrylamido-2-methyl-1-propanesulfonic acid. J Sci Food Agric 97:3831–3840. https://doi.org/10.1002/jsfa.8247
16. Mok CF, Ching YC, Muhamad F et al (2020) Adsorption of dyes using poly (vinyl alcohol)(PVA) and PVA-based polymer composite adsorbents: a review. J Polym Environ 28:775–793. https://doi.org/10.1007/s10924-020-01656-4
17. Jiang C, Wang X, Hou B, Hao C, Li X, Wu J (2020) Construction of a lignosulfonate–lysine hydrogel for the adsorption of heavy metal ions. J Agric Food Chem 68:3050–3060. https://doi.org/10.1021/acs.jafc.9b07540
18. Mok CF, Ching YC, Abu MF, Osman NA, Hai ND, Che Hassan CR (2020) Adsorption of dyes using poly (vinyl alcohol)(PVA) and PVA-based polymer composite adsorbents: a review. J Polym Environ 28:775–793. https://doi.org/10.1007/s10924-020-01656-4
19. Lei C, Bian Y, Zhi F, Hou X, Lv C, Hu Q (2022) Enhanced adsorption capacity of cellulose hydrogel based on corn stalk for pollutants removal and mechanism exploration. J Clean Prod 375:134130. https://doi.org/10.1016/j.jclepro.2022.134130
20. Duman O, Polat TG, Diker CÖ, Tunç S (2020) Agar/κ-carrageenan composite hydrogel adsorbent for the removal of methylene blue from water. Int J Biol Macromol 160:823–835. https://doi.org/10.1016/j.ijbiomac.2020.05.191
21. Alharby NF, Almutairi RS, Mohamed NA (2021) Adsorption behavior of methylene blue dye by novel crosslinked O-CM-Chitosan hydrogel in aqueous solution: kinetics, isotherm and thermodynamics. Polymers 13:3659. https://doi.org/10.3390/polym13213659
22. Junlapong K, Maijan P, Chaibundit C, Chantarak S (2020) Effective adsorption of methylene blue by biodegradable superabsorbent cassava starch-based hydrogel. Int J Biol Macromol 158:258–264. https://doi.org/10.1016/j.ijbiomac.2020.04.247
23. Wan X, Rong Z, Zhu K, Wu Y (2022) Chitosan-based dual network composite hydrogel for efficient adsorption of methylene blue dye. Int J Biol Macromol 222:725–735. https://doi.org/10.1016/j.ijbiomac.2022.09.21310.1016/j.ijbiomac.2022.09.213
24. Li Y, Liu SJ, Chen FM, Zuo JE (2019) High-strength apatite/attapulgite/alginate composite hydrogel for effective adsorption of methylene blue from aqueous solution. J Chem Eng Data 64:5469–5477. https://doi.org/10.1021/acs.jced.9b00616

Authors and Affiliations

Yunxiang Zheng[1] · Lina Zong[1] · Xiangpeng Wang[1]

✉ Xiangpeng Wang
wangxiangpeng1989@163.com

Yunxiang Zheng
zhengyunxiang1990@163.com

Lina Zong
000262@sdipct.edu.cn

[1] College of Chemical Engineering, Shandong Institute of Petroleum and Chemical Technology, 271 Beier Road, Dongying District, Dongying 257061, Shandong, China